Research Article

Chemical Review and Letters
journal homepage: www.chemrevlett.com
ISSN (online): 2645-4947 (print) 2676-7279

Bioactive potential and green synthesis of silver nanoparticles from Cucurbita pepo leaves: Antioxidant and antimicrobial activities

Nashmeel Hamad Ali[1,2], Awaz Faruq Abdullah[3], Safya Jamil Piro[3], Aryan Fathulla Qader[1,*], Abdalla Ali Amin[1,4], Abdulrahman Smail Ibrahim[5], Rebaz Anwar Omer[1,2], Musher Ismael Salih[1]

[1]*Department of Chemistry, Faculty of Science and Health, Koya University, 44023, Koya, Kurdistan Region – F.R. Iraq.*
[2]*Department of Pharmacy, College of Pharmacy, Knowledge University, 44001, Erbil, Iraq.*
[3]*Department of Chemistry, Faculty of Science, Soran University, 44008, Soran, Iraq.*
[4]*Department of Nursing, Raparin Technical and Vocational Institute, Rania, 46012, Sulaymaniyah, Kurdistan Region, Iraq.*
[5]*Department of Medical Laboratory Science, College of Science, Knowledge University, Erbil, Iraq.*

ARTICLE INFO

Article history:
Received 16 August 2025
Received in revised form 21 November 2025
Accepted 22 November 2025

Keywords:
Cucurbita pepo
Phytochemical
Antioxidant
Antibacterial
Silver nanoparticles

ABSTRACT

The present study investigates the phytochemical composition, vitamin content, and bioactive properties of *Cucurbita pepo* leaves, alongside their application in the green synthesis of silver nanoparticles (AgNPs). Ethanolic and acetone extracts of *Cucurbita pepo* leaves were analyzed for their total phenolic and flavonoid content, revealing significant antioxidant and metal-chelating activities, with ethanol proving to be the superior solvent. Chromatographic and spectrophotometric analyses identified a diverse profile of phenolic compounds and vitamins, including ascorbic acid and α-tocopherol. The green synthesis of AgNPs was achieved using these extracts, with nanoparticles characterized by UV-Vis, SEM, EDX, and XRD techniques, confirming their stability and crystalline structure. The synthesized AgNPs exhibited promising antibacterial activity against both Gram-positive (Staphylococcus aureus) and Gram-negative (Escherichia coli) bacteria, outperforming the crude extracts. This study highlights *Cucurbita pepo* leaves as a rich source of natural antioxidants, vitamins, and bioactive compounds with potential applications in nanotechnology with antimicrobial therapies.

1. Introduction

Plants have served as a cornerstone in traditional medicine, providing a source of natural compounds with pharmacological properties beneficial for human health [1, 2]. Among these, *Cucurbita pepo*, commonly known as pumpkin, holds significant attention due to its rich phytochemical profile [3]. Historically utilized in various cultural practices and traditional medicine, *Cucurbita pepo* is widely regarded for its nutritional and therapeutic benefits [4]. Both the seeds and flesh of *Cucurbita pepo* have been the subject of extensive research, highlighting their antioxidant, anti-inflammatory, and antimicrobial properties [5, 6].

However, its leaves are often overlooked despite their potential bioactive compounds, which may offer similar or even enhanced benefits [7]. The antioxidant properties of plant-based compounds are of particular interest in pharmacology and nutrition [8], as they play a crucial role in mitigating oxidative stress a contributor to various chronic diseases [9], including cardiovascular disease [10], cancer [11], and neurodegenerative disorders [9]. Oxidative stress results from an imbalance between free radicals and antioxidants in the body [12],

leading to cellular damage [13]. Phytochemicals, including phenolic acids and flavonoids, act as natural antioxidants by scavenging free radicals and offering a defense against oxidative damage [14]. *Cucurbita pepo* leaves are expected to contain significant amounts of these phytochemicals, making them promising candidates for antioxidant applications [15, 16]. Furthermore, phenolic compounds not only contribute to antioxidant capacity but also exhibit anti-inflammatory and antimicrobial activities, which may enhance the therapeutic potential of *Cucurbita pepo* leaves [17]. In addition to antioxidants, plant extracts have been recognized for their antimicrobial properties, providing a natural alternative to synthetic antimicrobial agents [18].

This is especially relevant given the increasing global

* Corresponding author E-mail: aryan.qader@koyauniversity.org
https://doi.org/10.22034/crl.2025.541558.1677
This work is licensed under Creative Commons license CC-BY 4.0

concern over antibiotic resistance [19], which has accelerated the search for alternative solutions to combat microbial infections [20]. Plant-derived antimicrobials, particularly those from medicinal plants, have shown efficacy against various pathogens, offering a sustainable and potentially less harmful solution to microbial infections [21]. Beyond their antioxidant and antimicrobial properties, *plant* leaves contain a range of vitamins, both water- and fat-soluble, that contribute to their health benefits [22]. Vitamins play essential roles in various biological processes, including immune function [23], skin health [24], and cellular repair [25]. The presence of water-soluble vitamins, such as vitamin C, and fat-soluble vitamins, such as vitamin E, further enhances the value of *Cucurbita pepo* as a source of nutrition and potential therapeutic applications [26]. The analysis of these vitamins is carried out using advanced analytical techniques, including high-performance liquid chromatography (HPLC), which enables precise identification and quantification of bioactive compounds [27]. In addition to HPLC, infrared (IR) spectroscopy [28] and other spectrophotometric methods [29] provide comprehensive insights into the phytochemical profile of the extracts, allowing for a detailed evaluation of their bioactive composition [30].

In recent years, the green synthesis of nanoparticles using plant extracts has emerged as an environmentally friendly approach to nanomaterial production [31]. Traditional methods of synthesizing silver nanoparticles often involve hazardous chemicals, posing risks to both the environment and human health [32]. Green synthesis, on the other hand, utilizes plant-based reducing agents, offering a sustainable and safer alternative [33]. The study of green-synthesized silver nanoparticles holds promise for applications in various fields, including medicine [34], agriculture [35], and environmental science [36], due to their unique properties and reduced environmental impact [37].

The aim of this study is to investigate the phytochemical composition, vitamin content, and bioactive properties of *Cucurbita pepo* leaves, with a specific focus on their antioxidant and antibacterial potential. Additionally, the study seeks to utilize these leaf extracts for the eco-friendly green synthesis and characterization of silver nanoparticles (AgNPs) and evaluate their effectiveness as antimicrobial agents. Through this research, the study aims to highlight the therapeutic and technological potential of *Cucurbita pepo* leaves in developing natural bioactive formulations and nanotechnology-based solutions for health and environmental applications.

2. Materials and Methods

2.1. Plant material and extraction

Cucurbita pepo leaves were harvested in October 2023 from the village of Shekhan, near the city of Soran in the Kurdistan Region of Iraq. The leaves were shade-dried and then ground into a fine powder for extraction. To identify the bioactive components, a conventional maceration extraction method was employed, using ethanol and acetone as solvents.

2.1.1. Maceration at room and high temperature

A total of 20.00 g of dried, ground leaves and fruits of *Cucurbita pepo* was extracted separately with 200 ml of ethanol and 200 ml of acetone, using conventional maceration. Each solvent extraction was performed for 24 hours, once at room temperature and once at elevated temperature. After extraction, the residue was removed by filtration. The filtrates were then concentrated by mixing and evaporating at 40 °C under 150 mbar pressure with a rotary evaporator. The extracts were completely dried in a vacuum oven and stored at 4-6 °C [38, 39, 40, 41].

2.2. Phytochemical study

Sample preparations involved dissolving 0.05 g of dried extracts in 5.0 mL of ethanol and 5.0 mL of acetone, followed by agitation for 30 minutes at room temperature in a water bath. These prepared solutions were then used to evaluate the antioxidant content of the samples.

2.2.1. Determination of total phenol content

The total phenolic content (TPC) in plant extracts was determined using the Folin-Ciocalteu colorimetric technique [42, 43]. A stock solution of gallic acid was prepared by dissolving 0.005 g of gallic acid in 5.0 mL of methanol and stirring in a water bath at room temperature for 30 minutes, followed by serial dilutions to create various concentrations. For the assay, 0.5 mL of each sample or standard was combined with 1.5 mL of distilled water and 0.25 mL of Folin-Ciocalteu reagent (1:1 with methanol). After vortexing for 5 minutes, 1.5 mL of 10% Na_2CO_3 solution was added, and the mixture was incubated in the dark for 1 hour at room temperature. Absorbance was measured at 760 nm using a UV-Vis spectrophotometer. A calibration curve was constructed using gallic acid at concentrations of (2.5, 5, 10, 20, 50, 100, and 150 ppm). The phenol contents are expressed as gallic acid equivalents per mg (mg GAE/g) of extract.

2.2.2. Determination of total flavonoid content

A standard calibration curve for total flavonoid content was generated using quercetin [44]. The stock solution of quercetin was prepared by dissolving 0.005 g of quercetin in 5.0 mL of methanol, followed by continuous stirring in a water bath at room temperature for 30 minutes. Serial dilutions in methanol were then used to prepare standard solutions with concentrations of (1, 5, 10, 20, 50, and 100 ppm). For the assay, 0.5 mL of each diluted quercetin standard or sample extract was mixed with 0.6 mL of 10% aluminum chloride, 0.1 mL of

1M sodium acetate trihydrate ($CH_3COONa \cdot 3H_2O$), and 2.7 mL of methanol. The mixture was thoroughly mixed and incubated at room temperature for 60 minutes. Absorbance was measured at 420 nm [45], with results expressed as mg QE/g dw (milligrams of quercetin equivalents per gram of dry weight).

2.3. Ferric reducing antioxidant power (FRAP) assay

The Ferric Reducing Antioxidant Power (FRAP) assay was conducted to measure the antioxidant capacity of extracts, based on their ability to reduce potassium ferricyanide [46]. In this assay, 0.5 ml of the sample or standard solution (quercetin) was mixed with 2.5 ml of 1% potassium ferricyanide ($K_3Fe(CN)_6$) and 2.5 ml of 0.2 M phosphate buffer (pH 6.6) in test tubes. The mixture was incubated for 30 minutes at 50 °C to allow ferricyanide $[Fe(CN)_6]^{3-}$ to be reduced to ferrocyanide $[Fe(CN)_6]^{4-}$. After incubation, 2.5 ml of 10% (w/v) trichloroacetic acid ($C_2HCl_3O_2$) was added to halt the reaction, followed by centrifugation at 3000 rpm for 10 minutes. Subsequently, 2.5 ml of the supernatant was mixed with 2.5 ml of distilled water and 0.5 ml of 0.1% $FeCl_3$ (ferric chloride) solution. A standard calibration curve was prepared using quercetin concentrations (15, 30, 50, 100, 150, 200, 300, 400, and 500 ppm) in methanol (0.005 g quercetin in 5 ml methanol). Absorbance was measured at 700 nm, and results were expressed as mg of quercetin equivalents per gram of dry weight (mg QE/g dw).

2.4. Metal chelating capacity (MCC) assay

The Metal Chelating Capacity (MCC) assay was conducted using a modified phenanthroline method to assess the chelating activity of the sample. In test tubes, 0.5 ml of the sample or standard solution (iron (II) sulfate) was combined with 2.5 ml of distilled water, 1 ml of $FeCl_3$ (ferric chloride), and 1 ml of phenanthroline. An additional 5.4 ml of distilled water was then added to the mixture. After thorough vortexing, the test tubes were incubated in the dark for 20 minutes. The results are expressed as iron (II) sulfate equivalents on a dry weight basis (mg Fe^{2+}/g dw). A standard calibration curve was prepared using iron(II) sulfate (0.02 g $FeSO_4 \cdot 7H_2O$ in 20 ml distilled water) with concentrations ranging from (10, 20, 50, 100, 150, and 200 ppm). Absorbance was measured at 510 nm using a UV-Vis spectrophotometer, and the results were reported as mg Fe^{2+} equivalents per gram of dry weight (mg Fe^{2+}/g dw) [47].

2.5. Chromatographic analysis of phenolic compounds in extracts

The phenolic composition of different extracts was analyzed by HPLC, following the method of Rodriguez Delgado et al. [48] with some modifications. Before injection, samples were filtered through a 0.45 µm Millipore membrane filter, with an injection volume of 50 µL. Separation was achieved using an ODS Hypersil 5 µm column (250×4 mm), protected by a LiChrospher 100 RP-18 guard column (5 µm, 4×4 mm). The mobile phase consisted of two solvents: solvent A (methanol-acetic acid-water, 10:2:88 v/v) and solvent B (methanol-acetic acid-water, 90:2:8 v/v), applied in a programmed gradient. Each sample was analyzed in duplicate. Compounds were identified by comparing the retention time and UV-Vis spectra with those of standards. Quantification was performed through external calibration using standards [49].

2.6. Determination of vitamins

2.6.1. Determination of vitamin C and MDA

The levels of malondialdehyde (MDA) and vitamin C were determined following the procedures of Karatepe [50]. The liquid-treated samples were first agitated with a syringe to ensure a uniform mixture. To each sample extract, 1 mL of 0.5 M $HClO_4$ was added to precipitate proteins and release MDA bound to amino groups and other compounds, along with 0.5 mL of distilled water, and mixed briefly using a vortex mixer. The samples were then centrifuged for 5 minutes, and the supernatant was collected. A 20 µL aliquot of this supernatant was injected into the HPLC instrument. The mobile phase consisted of 17.5% methanol and 85.5% potassium phosphate buffer (30 mM, pH 3.6) (v/v).

2.6.2. Determination of vitamin B and β-carotene

The liquid-soluble vitamins in the sample extracts were analyzed according to the procedures of Catignani and Bieri [51]. For each sample, 100 µL of extract was combined with 200 µL of ethanol, a 99:1 ratio of H_2SO_4, and 100 µL of distilled water in a test tube to precipitate proteins. The samples were mixed and centrifuged at 4500 rpm for 5 minutes. After centrifugation, 100 µL of n-hexane containing 0.05% BHT was added to extract the lipid-soluble vitamins. This mixture was again mixed and centrifuged, and the resulting hexane layer was transferred to a separate test tube. An additional 100 µL of n-hexane was added to the remaining sample, mixed, centrifuged, and combined with the previous hexane layer. The hexane layer was then evaporated under nitrogen gas, and the residue was dissolved in 50 µL of methanol, 25 µL of acetonitrile, and 25 µL of chloroform. Finally, 20 µL of this solution was injected into the HPLC instrument. The mobile phase consisted of methanol, acetonitrile, and chloroform in a 47:42:11 ratio (v/v).

2.7. Green synthesis and characterization of AgNPs from extracts

Silver nanoparticles (AgNPs) were synthesized using ethanol and acetone extracts of *Cucurbita pepo* leaves. A 1

mM aqueous solution of silver nitrate ($AgNO_3$) was prepared. Then, 300 mg of each extract (ethanol or acetone) was dissolved in a small amount of the corresponding solvent and diluted to a final volume of 100 ml with water.

To initiate the reaction, 60 ml of the prepared *Cucurbita pepo* extract solution was mixed with 10 ml of the silver nitrate solution. The mixture was kept at room temperature to allow the synthesis reaction to proceed [52].

The bioreduction of $AgNO_3$ was confirmed by scanning the UV-Vis spectra of the reaction mixture, which showed an absorption maximum within the wavelength range of 200–700 nm, using a Thermo Scientific UV spectrophotometer. Additionally, the bioreduced reaction mixture was analyzed by scanning electron microscopy (SEM) using a JEOL Model JFC-1600.

2.8. Antimicrobial activity of extracts, and AgNPs

The antibacterial potential of the ethanol and acetone extracts, along with the synthesized AgNPs, was evaluated at varying concentrations of (150, 250, 350 mg) using the well diffusion method against various bacteria Staphylococcus aureus (G+) and Escherichia coli (G-) bacteria [53].

2.9. Infrared spectroscopy (IR) analysis of extracts, and AgNPs

Infrared Spectroscopy (IR) was employed to analyze the acetone and ethanol extracts of *Cucurbita pepo* leaves as well as the synthesized silver nanoparticles (AgNPs). The IR spectra were recorded within the wavelength range of 4000 to 500 cm^{-1}. This analysis aimed to identify the functional groups present in the plant extracts and confirm their role in reducing and stabilizing the AgNPs [54].

3. Results and Discussion

The extraction of 20 g of *Cucurbita pepo* leaf material with ethanol and acetone yielded 1.304 g and 0.746 g of dry residue, respectively. The percentage yields were calculated as 6.53% for the ethanolic extract and 3.73% for the acetone extract.

3.1. Polyphenolic compounds

Phenolic and flavonoid compounds are well-recognized for their extensive health benefits, including antiviral, anti-allergic, antiplatelet, anti-inflammatory, anticancer, and antioxidant properties [55].

In this study, the ethanol extract of *Cucurbita pepo* leaves demonstrated a significantly higher phytochemical content compared to the acetone extract, as shown in (Table 1), highlighting the superior extraction efficiency of ethanol. The total phenolic content (TPC) in the ethanol extract (10.043 mg GAE/g) was markedly higher than in the acetone extract (2.878 mg GAE/g), underscoring the strong antioxidant activity of phenolic compounds. Similarly, the total flavonoid content (TFC) in the ethanol extract (5.28 mg QE/g) surpassed that of the acetone extract (2.42 mg QE/g), confirming ethanol's efficiency in isolating flavonoids, another key class of antioxidant compounds.

These findings align with previous reports of *C. pepo* leaf extracts prepared with ethyl acetate, a solvent known for its flavonoid extraction capacity, which yielded TPC and TFC values of 32.6 ± 0.17 mg GAE/g and 80.5 ± 0.02 mg RUE/g, respectively [56].

However, the lower TPC and TFC observed in this study could be attributed to differences in solvents and experimental conditions. Phenolic and flavonoid content variations across solvents are likely due to their high solubility in polar solvents like ethanol and aqueous solutions, while less polar solvents like acetone exhibit lower extraction efficiency [57].

The elevated levels of phenolics and flavonoids in the ethanol extract enhance its functional and antioxidant potential, supporting ethanol as a superior solvent for bioactive compound extraction.

3.2. Antioxidant activities

Improved extraction of phenolic and flavonoid compounds enhances the reducing properties of the extract, a key indicator of antioxidant activity. The antioxidant capacity of these compounds arises from their redox properties, enabling them to neutralize free radicals, quench reactive oxygen species, and decompose peroxides. The Fe(III) reduction assay measures electron-donating activity, a crucial mechanism of antioxidant function [58, 59].

The ethanol extract exhibited a significantly higher ferric reducing antioxidant power (FRAP) of 43.45 mg QE/g compared to 12.1 mg QE/g for the acetone extract (Table 1), reflecting its robust reducing ability. Previous studies on *C. pepo* fruit extracts using water-organic solvent mixtures reported exceptionally high FRAP values (4295.8–5164.2 μmol Fe(II)/g of dry sample). In contrast, this study's ethanol extract of *C. pepo* leaves, while demonstrating superior antioxidant capacity compared to acetone, exhibited relatively weaker reducing activity.

This suggests that the plant part (leaves vs. fruit) and its phytochemical composition may influence antioxidant efficiency.

Metal chelating activity (MCC) of various pumpkin cultivars, including *C. pepo*, underscores the role of antioxidants in mitigating oxidative stress by chelating metal ions like iron. Iron chelation inhibits the Fenton reaction, preventing hydroxyl radical formation that disrupts redox balance [60].

The ethanol extract of *C. pepo* leaves showed

significantly higher MCC (569.69 mg Fe^{2+}/g) compared to the acetone extract (330 mg Fe^{2+}/g) (Table 1).

These results are consistent with previous studies showing that pumpkin extracts possess notable iron chelating activity, with methanol-water mixtures being particularly effective, as observed in cultivars like 'Casperita' (12056.12 µg EDTA/100 g dm) and 'Delicata' (11081.85 µg EDTA/100 g dm). Even water extracts showed moderate activity, such as in 'Butterkin' (8169.37 µg EDTA/100 g dm), emphasizing solvent choice as a determinant of chelating efficiency.

The superior performance of the ethanol extract in this study highlights its effectiveness in extracting bioactive compounds with strong metal-binding properties, mitigating metal-catalyzed oxidative damage. These findings reinforce ethanol's utility as a solvent and the antioxidant potential of *C. pepo* leaf extracts as a valuable source of natural chelating agents.

3.3. Phenolic profile analysis

The chromatographic analysis of phenolic compounds in *Cucurbita pepo* leaf extracts was conducted using HPLC, with the results presented for the standard compounds, acetone extract and ethanol extract. The phenolic profile of the *Cucurbita pepo* leaf extracts showed a wide range of phenolic acids and flavonoids, which are well-known for their antioxidant and health-promoting properties.

In (Table 2), the standard compounds showed high recovery rates, with values ranging from 93% to 99%, confirming the reliability and accuracy of the HPLC method used. The concentrations of each compound in the standard solution were consistent with the expected values, which is crucial for comparing the extracts.

For the acetone extract (Table 3), notable compounds included rutin, p-coumaric acid, luteolin, and caffeic acid, with concentrations of 30.26 µg/mL, 36.56 µg/mL, 54.12 µg/mL, and 99.39 µg/mL, respectively. The higher concentration of luteolin and caffeic acid in the acetone extract suggests that acetone is a more effective solvent for extracting flavonoids and phenolic acids that have antioxidant properties.

In (Table 4), the ethanol extract showed an even greater concentration of certain compounds, particularly caffeic acid (119.31 µg/mL) and luteolin (68.08 µg/mL), which were significantly higher than in the acetone extract.

This suggests that ethanol is an even better solvent for extracting these bioactive compounds from *Cucurbita pepo* leaves. The ethanol and acetone extract showed a high recovery rate, ranging from 93% to 101%, confirming the consistency and reliability of the extraction processes.

The presence of various phenolic compounds, such as gallic acid, catechin, and quercetin, in both extracts further supports the idea that *Cucurbita pepo* leaves are rich in bioactive compounds with potential health benefits, including antioxidant and anti-inflammatory properties. These compounds have been linked to the reduction of oxidative stress and the prevention of various chronic diseases.

HPLC Chromatogram visually demonstrate the presence of phenolic compounds in the extracts, with distinct peaks corresponding to various compounds, thus confirming the successful extraction of bioactive phenolics from *Cucurbita pepo* leaves (Figure 1).

Table 1 Phytochemical composition and antioxidant capacities of *Cucurbita pepo* leaf extracts in acetone and ethanol: total phenolic and flavonoid content, FRAP, and metal chelating capacity.

Extract	TPC (mg GAE/g)	TFC (mg QE/g)	FRAP (mg QE/g)	MCC (mg Fe^{2+}/g)
Cucurbita pepo leaf acetone extract	2.8787±0.5	2.42±0.08	12.1±0.0578	330±0.578
Cucurbita pepo leaf ethanol extract	10.043±0.06	5.28±0.824	43.45±0.07	569.69±0.635

Table 2. HPLC chromatogram of standard phenolic compounds (concentration and recovery data).

Peak IDs	RT (min)	Peak area (%)	Recovery (%)	Concentration (µg/mL)
Gallic acid	3.43	7.907545	95	20.00±0.00
p-hydroxybenzoic acid	4.05	6.224513	98	20.00±0.00
Catechin	4.31	5.947688	97	20.00±0.00
Epicatechin	5.26	7.52604	96	20.00±0.00
Rutin	7.21	7.558384	93	20.00±0.00
m-Coumaric acid	10.18	7.919092	99	20.00±0.00
Myricetin	11.59	8.025663	97	20.00±0.00
Quercetin	13.71	7.185664	96	20.00±0.00
Caffeic acid	14.23	6.860155	96	20.00±0.00
Luteolin	14.45	5.944195	99	20.00±0.00
Chlorogenic acid	15.19	7.28173	94	20.00±0.00
Apigenin	16.28	7.748684	97	20.00±0.00
Kaempferol	18.11	6.732013	93	20.00±0.00

Table 3. HPLC chromatogram of phenolic compounds in *Cucurbita pepo* leaf acetone extract.

Peak IDs	RT (min)	Peak area (%)	Recovery (%)	Concentration(µg/mL)
Gallic acid	3.44	8.424523	97	18.31865
P-OH-Benzoic Acid	4.04	5.035609	97	10.94965
Catechin	4.31	4.327198	99	4.704624
Epicatechin	5.25	5.001701	96	5.437959
Rutin	7.21	9.277162	98	30.259
p-Coumaric acid	10.18	11.20793	101	36.55651
Myricetin	11.59	5.57547	100	12.12354
Quercetin	13.71	4.369238	98	4.750331
Caffeic acid	14.22	18.28351	100	99.39116
Luteolin	14.45	12.44411	101	54.11801
Chlorogenic acid	15.20	4.426333	97	4.812406
Apigenin	16.28	7.307602	100	15.88997
Kaempferol	18.11	4.319618	98	4.696383

Table 4. HPLC chromatogram of phenolic compounds in *Cucurbita pepo* leaf ethanol extract.

Peak IDs	RT (min)	Peak area (%)	Recovery (%)	Concentration(µg/mL)
Gallic acid	3.44	8.997929	97	22.64372
P-OH-Benzoic Acid	4.04	4.609335	97	11.59961
Catechin	4.31	4.048156	99	5.093688
Epicatechin	5.25	4.573398	96	5.754587
Rutin	7.21	9.597769	98	36.22986
p-Coumaric acid	10.18	9.690237	101	36.57891
Myricetin	11.59	6.158977	100	15.49936
Quercetin	13.71	3.898782	98	4.905736
Caffeic acid	14.22	18.9648	100	119.3145
Luteolin	14.45	13.52583	101	68.07678
Chlorogenic acid	15.20	4.25421	97	5.35296
Apigenin	16.28	7.295847	100	18.36035
Kaempferol	18.11	4.384734	98	5.517196

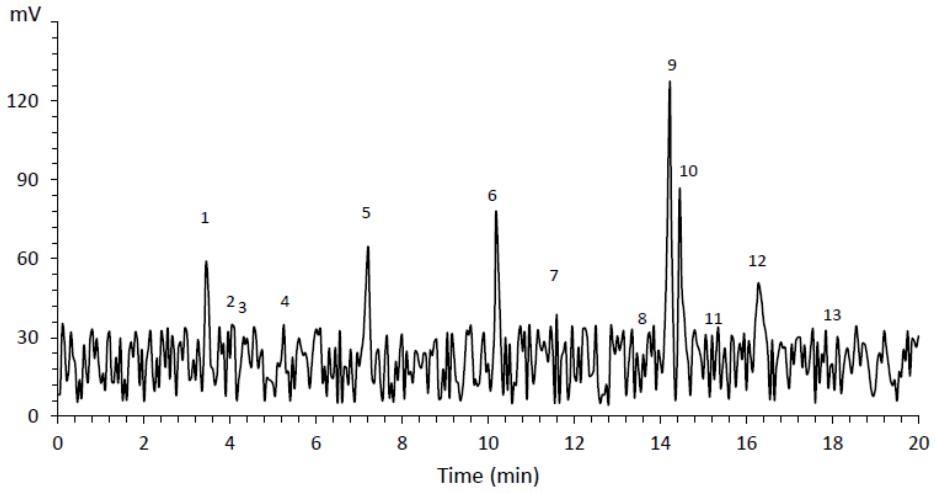

Fig. 1. HPLC chromatogram for acetone and ethanol leaf extracts

3.4. Vitamin profile

Vitamins in plant extracts are essential for overall health, offering benefits such as enhanced immunity, improved skin health, and increased energy production. Their natural synergy with antioxidants and phytonutrients boosts absorption and provides added protection against oxidative stress and chronic diseases [61]. An analysis of water-soluble vitamins in *Cucurbita pepo* leaf extracts revealed variations between acetone and ethanol as extraction solvents (Table 5). Ethanol extracts had higher concentrations of ascorbic acid (119.3 µg/100g) compared to acetone extracts (98.8 µg/100g), suggesting that ethanol's solvent properties are more effective for vitamin C extraction. Other vitamins, such as thiamine, niacin, and riboflavin, also showed higher concentrations in ethanol extracts, further supporting its efficiency for extracting hydrophilic compounds. For fat-soluble vitamins and oxidative stress markers (Table 6),

both extracts contained significant amounts of α-tocopherol, but ethanol extracts demonstrated a higher concentration (2.35 mg/g) compared to acetone extracts (1.23 mg/g), highlighting ethanol's effectiveness in extracting this potent antioxidant. Similarly, carotenoid content was higher in ethanol extracts (701.1 µg/g) than in acetone (598.9 µg/g). Interestingly, both extracts contained malondialdehyde (MDA), a marker of oxidative stress, with slightly higher levels in the acetone extract (55.1 nmol/g) compared to ethanol (48.8 nmol/g), indicating acetone might extract more compounds associated with oxidative damage. Despite limited research on the vitamin content of *Cucurbita pepo* leaves, studies on its seeds and pulp provide additional insights. Srbinoska et al., reported high tocopherol content in Cucurbita pepo seeds (117.81 mg/kg), underscoring their richness in vitamin E [62]. Similarly, Kulczyński and Gramza-Michałowska, found significant amounts of vitamin C (41.98–82.89 mg/100g dry mass), thiamine (0.15–0.72 mg/100g dry mass), and tocopherols, including alpha-tocopherol (1.69–6.44 mg/100g dry mass) and gamma-tocopherol (0.68–8.07 mg/100g dry mass), in Cucurbita pepo pulp [63]. Together, these findings illustrate the diverse vitamin content across different parts of the plant, with seeds, pulp, and leaves serving as particularly nutrient-dense sources.

The HPLC chromatograms in (Figure 2 and 3) further illustrate the clear distinctions between the extracts. These figures confirm the presence and concentration of the various compounds, further supporting the interpretation that ethanol is a more effective solvent for extracting vitamins and antioxidants from *Cucurbita pepo* leaves.

3.5. Green silver nanoparticle fabrication and analysis

Silver nanoparticles (AgNPs) were synthesized using ethanol and acetone extracts of Cucurbita pepo leaves with a 1 mM $AgNO_3$ solution. The reaction was confirmed by UV-Vis spectroscopy, and the nanoparticles were characterized using SEM, Energy Dispersive X-ray Spectroscopy (EDX), X-ray Diffraction (XRD) analysis, and band gap studies.

Table 5. Water-soluble vitamin content in *Cucurbita pepo* leaf extracts (acetone and ethanol extracts).

Extracts	Ascorbic Acid (µg/100g)	Thiamine (µg/100g)	Niacin (µg/100g)	Pantothenic Acid (µg/100g)	Folic Acid (µg/100g)	Biotin (µg/100g)	Riboflavin (µg/100g)
Acetone extract	98.84296	5.576174	3.39262	11.43109	18.50854	4.540683	38.43111
Ethanolic extract	119.2979	8.247419	3.775547	15.22078	23.833552	6.078905	47.97897

Table 6. Fat-soluble vitamin and MDA content in *Cucurbita pepo* leaf extracts (acetone and ethanol extracts).

Extracts	Retinyl acetate (mg/g)	Cholecalciferol (mg/g)	α-tocopherol (mg/g)	Carotenoids (µg/g)	MDA (nmol /g)
Acetone extract	0.401979	ND	1.226534	598.8846217	55.09788625
Ethanolic extract	0.551245	ND	2.352267	701.0750967	48.75511792

* ND = not detected.

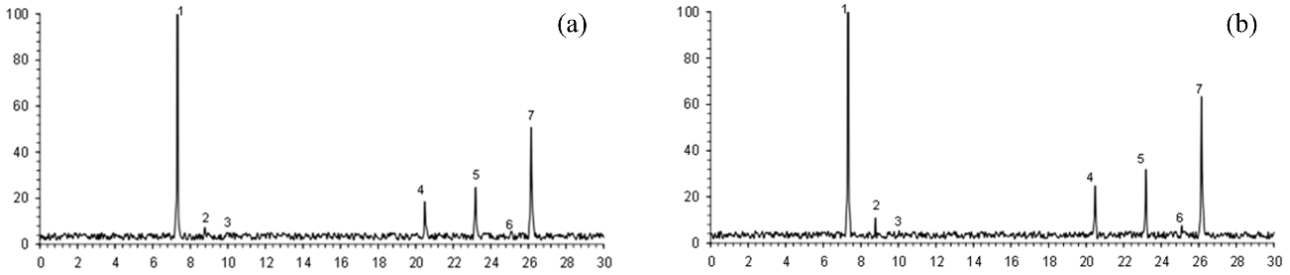

Fig. 2. HPLC chromatograms of water-soluble vitamins in *Cucurbita pepo* leaf extracts: (a) acetone, (b) ethanol extracts.

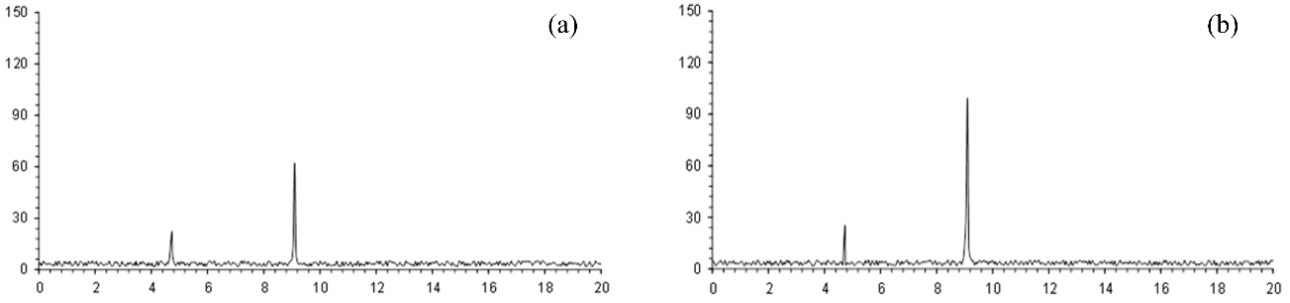

Fig. 3. HPLC chromatograms of fat-soluble vitamins in *Cucurbita pepo* leaf extracts: (a) acetone, (b) ethanol extracts.

Silver nanoparticles (AgNPs) are widely used in biotechnology and biomedical fields. Traditional chemical and physical synthesis methods often involve toxic chemicals, posing risks to living organisms. To address this, green chemistry-based biological methods have been developed, utilizing resources such as bacteria, fungi, enzymes, and plant extracts [64]. Green synthesis of AgNPs involves three key steps: selecting a solvent medium, an environmentally friendly reducing agent, and non-toxic stabilizing substances. Among these methods, plant extract-based synthesis is preferred for its simplicity, elimination of cell culture maintenance, and scalability for large-scale production [64, 65].

3.5.1. SEM and FESEM of synthesized AgNPs

The field emission scanning electron microscope (FESEM) image of biogenically synthesized AgNPs revealed a mixture of small spherical nanoparticles along with larger triangular and elliptical silver nanoparticles, consistent with the results obtained from scanning electron microscopy (SEM) analysis (Figure 4).

These nanoparticles exhibited varying nano-diameters. The sample synthesized using Cucurbita pepo leaf extract showed highly agglomerated nanoparticles, forming large aggregates. In some cases, the nanoparticles appeared bulked, possibly due to crosslinking or solvent evaporation during sample preparation [66].

3.5.2. Energy dispersive x-ray spectroscopy (EDX) of synthesized AgNPs

Energy Dispersive X-ray (EDX) analysis provided detailed information about the elemental composition of the synthesized AgNPs. The analysis revealed strong signals for silver (77.09%), along with smaller contributions from carbon (8.8%), oxygen (1.85%), and sodium (3.24%), with no impurities or additional elements detected, confirming the high purity of the nanoparticles (Table 7; Figure 5a). The reduction of metallic silver was stabilized by alkyl chains, as indicated by the presence of carbon and oxygen in the EDX analysis. Additionally, a distinct peak observed near ~3 keV, characteristic of biosynthesized AgNPs [67].

3.5.3. X-ray diffraction analysis (XRD) of synthesized AgNPs

X-Ray Diffraction (XRD) analysis was performed to determine the crystal structure of the AgNPs. Four distinct peaks were observed at 33.7°, 38.1°, 44.43°, and 64.3°, corresponding to the (122), (111), (200), and (220) lattice planes, respectively, confirming a face-centered cubic (FCC) structure (Figure 5b).

The high-intensity peaks indicated the polycrystalline nature of the nanoparticles. The sharp peak at 38.1° (reflection index (111)) aligns with the values reported by the Joint Committee on Powder Diffraction Standards, further confirming the cubic crystalline nature of the AgNPs. Using the Debye-Scherrer formula, the average size of the AgNPs was calculated to be 14.32 nm [67].

3.5.4. UV-Visible spectroscopy of synthesized AgNPs

The Surface Plasmon Resonance (SPR) vibration observed at 424 nm confirms the synthesis of AgNPs, as illustrated in (Figure 6b). This finding aligns with previous studies, such as Shankar et al., which reported AgNPs absorption within the range of 410–440 nm, attributed to their SPR properties [68].

Additionally, the aqueous leaf extract spectrum exhibited peaks at 260, 325, and 385 nm, which were associated with the presence of phytochemicals, including alkaloids and flavonoids (Figure 6a). These observations are consistent with reports by Rojas et al., who attributed similar absorption peaks to phenolic groups like alkaloids and flavonoids [69].

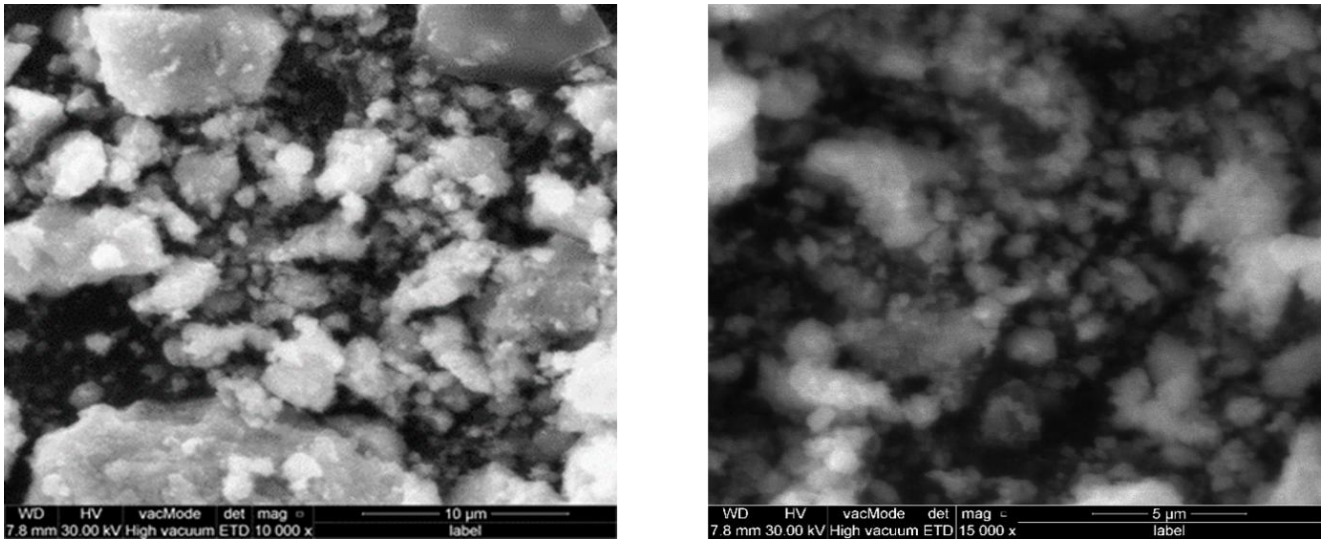

Fig. 4. The SEM micrograph obtained for the synthesized silver nanoparticles.

Table 7. EDX analysis of synthesized AgNPs (elemental profile).

Element	Lines	Mass %
Silver	L-Serie	77.09488561
Oxygen	K-Serie	10.85196855
Carbon	K-Serie	8.807118117
Sodium	K-Serie	3.246027722

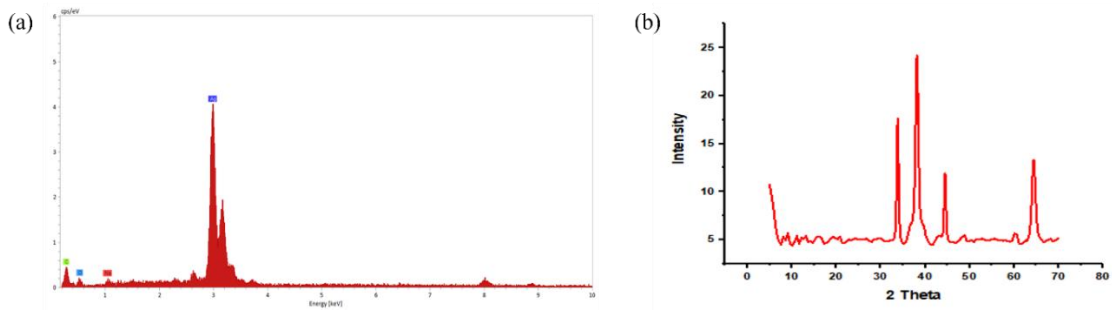

Fig. 5. Analysis of synthesized AgNPs: (a) EDX spectra and elemental profile, (b) XRD pattern.

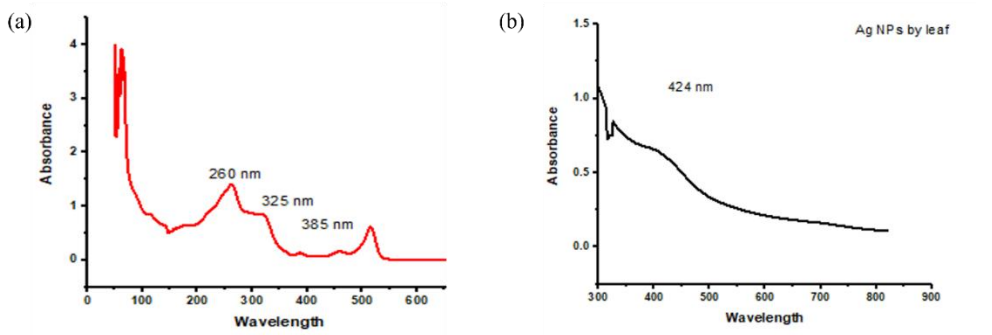

Fig. 6. UV–vis spectrum: (a) Extract of *Cucurbita pepo* leaves, (b) AgNPs synthesized using extract of *Cucurbita pepo* leaves.

3.5.5. Band gap study of synthesized AgNPs

Using Tauc's formula, the direct band gap of the synthesized AgNPs was calculated as 2.57 eV, a value consistent with previous findings on AgNPs. This low energy requirement for electron excitation aligns with the observed optical properties, where significant contributions stem from transitions at the fundamental absorption edge [70]. The result not only supports earlier studies but also highlights the potential of these AgNPs in applications where efficient photon-electron interactions are essential (Figure 7).

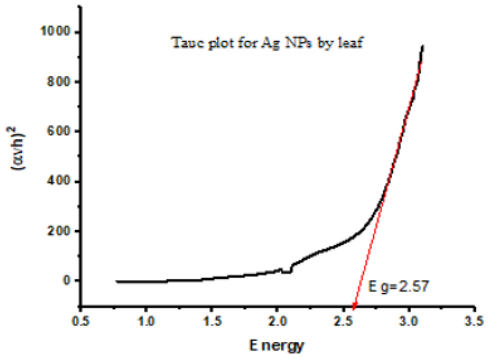

Fig. 7. Optical bandgap determination of AgNPs via Tauc plot.

This agreement between theoretical insights and the experimental band gap value demonstrates the utility of synthesized AgNPs in optical and electronic applications.

3.6. Bacterial inhibition potential

Various extracts exhibit different antimicrobial effects based on their active compounds. Ethanol extract, in particular, is highly effective against bacteria due to its ability to efficiently extract phenolic components [71].

A study investigated the antibacterial properties of ethanol and acetone extracts derived from Cucurbita pepo leaves against Staphylococcus aureus (Gram-positive) and Escherichia coli (Gram-negative) at concentrations of 150 mg/ml, 250 mg/ml, and 350 mg/ml (Figure 8).

The results indicated that the extracts did not produce any significant inhibition zones. These findings are consistent with those of Break et al., who also reported that extracts from mature C. pepo leaves demonstrated no significant antibacterial activity against either bacterium [17].

Notably, silver nanoparticles (AgNPs) synthesized from these extracts exhibited clear antibacterial activity, with inhibition zones of 11 mm for E. coli and 14 mm for S. aureus. At a concentration of 250 mg/ml, similar antimicrobial resistance was observed, with AgNPs

maintaining inhibition zones of 11 mm and 14 mm against E. coli and S. aureus, respectively.

At the highest concentration of 350 mg/ml, the extracts continued to inhibit both E. coli and S. aureus, with AgNPs showing slightly larger inhibition zones of 12 mm for E. coli while maintaining a 14 mm zone for S. aureus (Table 8).

These results are consistent with a previous study by Roy et al. [72], which reported inhibition zones of 11.43 ± 2.15 mm for pumpkin nanoparticles against S. aureus [73]. Ethanol extract remains particularly effective against bacteria due to its phenolic content (Amin et al., 2017).

3.7. Infrared characterization of extracts and AgNPs

Infrared spectroscopy is a valuable tool for identifying functional groups attached to the flavonoid molecule's core structure. Molecules absorb infrared radiation through transitions between specific energy levels, particularly vibrational energy levels within the 4000 to 500 cm^{-1} range.

This absorption causes chemical bonds to stretch and bend, and an IR spectrophotometer measures these absorptions, as shown in (Figure 9), with results in (Table 9). Strong bands between 4000-3000 cm^{-1} and 3550-3200 cm^{-1} indicate hydroxyl group vibrations, signaling the presence of polyphenolic compounds.

The band at 2000-1650 cm^{-1} corresponds to the stretching vibrations of C-H bending within a conjugated double bond system, typical of aromatic compounds. These findings align with results from ignition tests. Additionally, the band between 1275-1200 cm^{-1} indicates the presence of a dialkyl ether group (C-O-C bridge), suggesting an aromatic ether compound [74, 75].

Analysis of individual extracts revealed that ethanol is generally a more effective solvent due to the C=O groups in the extract components.

Stability testing of the nanoparticles showed them to be stable for over four weeks, with no notable wavelength shift, likely due to antioxidant phytochemicals adhering to the nanoparticles' surfaces and preventing degradation. Figure 9 displays FT-IR signals of silver nanoparticles (AgNPs) synthesized from *Cucurbita pepo* plant extract, with major vibrations at approximately 3550 cm^{-1} (OH) [70], 1745 cm^{-1} (C=O) [76], and 1435–1575 cm^{-1} (C=C aromatic ring) [77]. These signals confirm the presence of plant-derived phytochemicals on the AgNP surfaces, contributing to their stability and protective qualities.

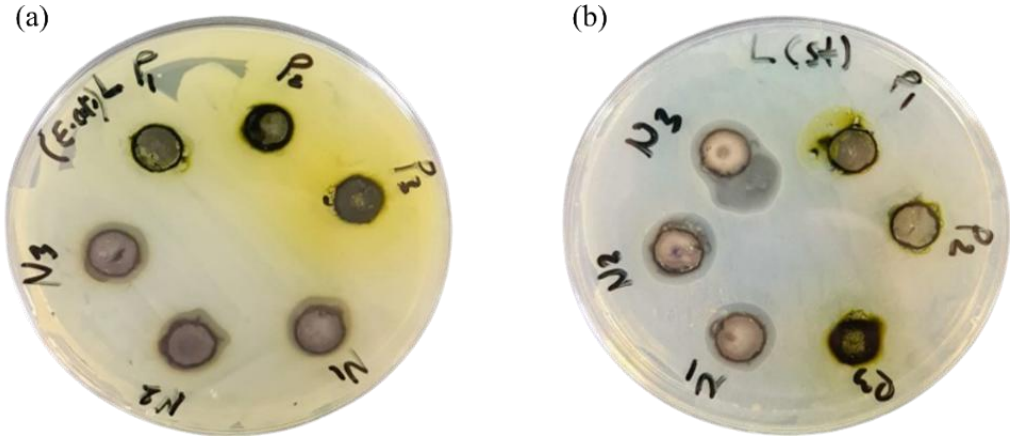

Fig. 8. Antibacterial activity of AgNPs of *Cucurbita pepo* leaves at different concentrations (150, 250, 350mg) against (a) Staphylococcus aureus (G+), (b) Escherichia coli (G-) bacteria.

Table 8. Antibacterial activity of acetone and ethanol extracts and AgNPs of *Cucurbita pepo* leaves at different concentrations (150, 250, 350mg) against Staphylococcus aureus (G+) and Escherichia coli (G-) bacteria, with zone of inhibition in mm.

Bacterial Strains	Acetone, Ethanol extracts	AgNPs
	Concentrations (150mg)	
E. coli	Resistance	11mm
Staphylococcus aureus	Resistance	14mm
	Concentrations (250mg)	
E. coli	Resistance	11mm
Staphylococcus aureus	Resistance	14mm
	Concentrations (350mg)	
E. coli	Resistance	12mm
Staphylococcus aureus	Resistance	14mm

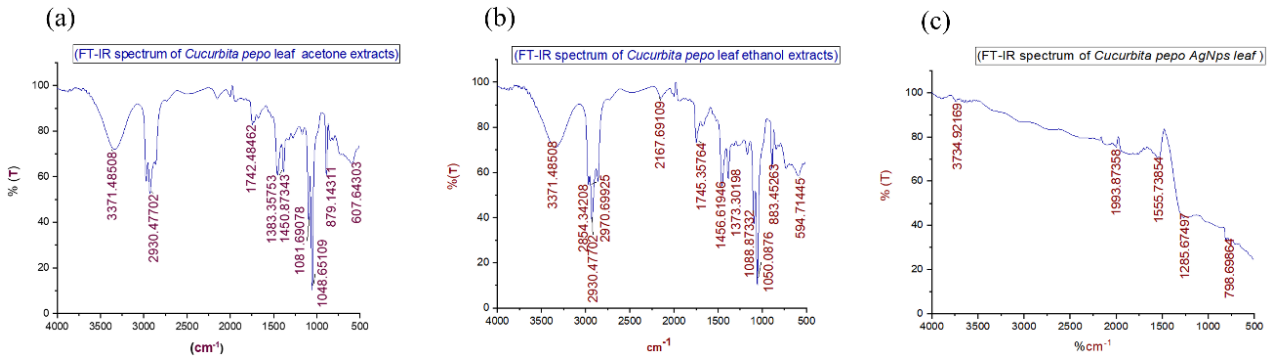

Fig. 9. FTIR spectrum of *Cucurbita pepo* leaf extracts: (a) acetone, (b) ethanol, and **(c)** AgNps.

Table 9. infrared absorption peaks and its related functional groups of Pig. for *Cucurbita pepo* leaf extracts (acetone, ethanol, and AgNps).

Bond frequency cm^{-1}	Group or class	Bond shape	Assignment of remark [78]
4000-3000	O-H	(M- Sh)	Stretching alcohol
3550-3200	O-H stretching	Strong, Broad	Alcohol
34345-3435	NH Stretching	M	Amides
3100-3000	C-H stretching	M	Alkene
2200 -2100	C≡C	Sh	Alkynes
2000-1650	C-H bending	W	Aromatic compound
1725-1705	C=O stretching	S	Aliphatic ketone
1500-1400	c-c in ring	M	Ar c-c stretch
1275-1200	C-O stretching	S	Alkyl aryl ether
1250-1020	C-N stretching	M	Amine
1150-1085	C-O stretching	S	Aliphatic ether
950-910	RCO-OH O-H bend	M	Carboxylic acid
690-515	C-Br stretching	S	Halo compound

W: weak, Sh: sharp, M: medium, Br: broad, S: strong.

4. Conclusion

This study demonstrates that *Cucurbita pepo* leaves are a valuable source of bioactive compounds, including phenolics, flavonoids, and essential vitamins, which contribute to their notable antioxidant properties. Ethanolic extracts proved superior in extracting these bioactive compounds compared to acetone extracts, emphasizing the importance of solvent selection in maximizing phytochemical yields. The green synthesis of silver nanoparticles (AgNPs) using these extracts offers an eco-friendly alternative to conventional nanoparticle synthesis methods. The synthesized AgNPs exhibited strong antibacterial activity against Staphylococcus aureus and Escherichia coli, highlighting their potential in antimicrobial applications. These findings underscore the therapeutic and technological potential of *Cucurbita pepo* leaves, suggesting their use in developing natural antioxidant formulations and nanotechnology-based antimicrobial agents. Future studies could explore scaling up nanoparticle production and evaluating the pharmacological applications of these extracts and AgNPs in vivo.

Acknowledgements

The authors would like to express their gratitude to the Head of the Chemistry Department at Koya University in Iraq for providing laboratory facilities.

References

[1] S.C. Izah, O.I. Ogidi, M.C. Ogwu, S.S. Salimon, Z.M. Yusuf, M. Akram, et al., Historical perspectives and overview of the value of herbal medicine. *Herbal Medicine Phytochemistry: Applications and Trends*, (2024) 3-35.

[2] M.A. Eruaga, E.O. Itua, J.T. Bature, Exploring herbal medicine regulation in Nigeria: Balancing traditional practices with modern standards. *GSC Adv. Res. Rev.*, 18 (2024) 083-90.

[3] S.E. Badr, M. Shaaban, Y.M. Elkholy, M.H. Helal, A.S. Hamza, M.S. Masoud, et al., Chemical composition and biological activity of ripe pumpkin fruits (Cucurbita pepo L.) cultivated in Egyptian habitats. *Nat. Prod. Res.*, 25 (2011) 1524-39.

[4] M. Adnan, S. Gul, S. Batool, B. Fatima, A. Rehman, S. Yaqoob, et al., A review on the ethnobotany, phytochemistry, pharmacology and nutritional composition of Cucurbita pepo L. *J. Phytopharmacol.*, 6 (2017) 133-9.

[5] M. Peng, D. Lu, J. Liu, B. Jiang, J. Chen, Effect of roasting on the antioxidant activity, phenolic composition, and nutritional quality of pumpkin (Cucurbita pepo L.) seeds. *Front. Nutr.*, 8 (2021) 647354.

[6] H.F. Ayyildiz, M. Topkafa, H. Kara, Pumpkin (Cucurbita pepo L.) seed oil. *Fruit Oils: Chemistry and Functionality*, (2019) 765-88.

[7] D. Hu, W. Si, W. Qin, J. Jiao, X. Li, X. Gu, et al., Cucurbita pepo leaf extract induced synthesis of zinc oxide nanoparticles, characterization for the treatment of femoral fracture. *J. Photochem. Photobiol. B*, 195 (2019) 12-6.

[8] E.D.N.S. Abeyrathne, K. Nam, X. Huang, D.U. Ahn, Plant-and animal-based antioxidants' structure, efficacy, mechanisms, and applications: A review. *Antioxidants*, 11 (2022) 1025.

[9] R. Chandran, H. Abrahamse, Identifying Plant-Based Natural Medicine against Oxidative Stress and Neurodegenerative Disorders. *Oxid. Med. Cell. Longev.*, 2020 (2020) 8648742.

[10] a) M. Sedighi, M. Bahmani, S. Asgary, F. Beyranvand, M. Rafieian-Kopaei, A review of plant-based compounds and medicinal plants effective on atherosclerosis. *J. Res. Med. Sci.*, 22 (2017) 30. b) V.R. Battula, S.S. Kaladi, L.P. Yandrati, P.K. Edigi, S. Bujji, V. Nasipireddy, et al., Synthesis, Anticancer Evaluation and Molecular Docking studies of Novel Benzophenone based 1,2,3-Triazole Hybrids. *J. Chem. Lett.*, 5 (2024) 236-248. doi: 10.22034/jchemlett.2024.474931.1225 c) D.T. Sakhare, Synthesis of Schiff Bases Ligand And Biological Activities of Their Transition Metal Complexes. *J. Chem. Technol.*, 1 (2025) 189-195. doi: 10.22034/jchemtech.2025.555817.1029 d) Y. Hassan, A.S.S. Sovogui, M. Kabir, H.D. Hassan, Synthesis, Antimicrobial Activity and Docking Studies of Biarylhydrazones. *Med. Med. Chem.*, 2 (2025) 18-24. doi: 10.22034/medmedchem.2025.511259.1028

[11] a) S. Prakash, Radha, M. Kumar, N. Kumari, M. Thakur, S. Rathour, et al., Plant-based antioxidant extracts and compounds in the management of oral cancer. *Antioxidants*, 10 (2021) 1358. b) A.B. Bilyaminu, M.Y. Abubakar, D. Abubakar, Green Organic Synthesis in Drug Development: Advances in Enzyme- and Microorganism-Mediated Processes. *Med. Med. Chem.*, 1 (2024) 115-128. doi: 10.22034/medmedchem.2024.489545.1017 c) P.V. Patale, S.R. Mathapati, J.L. Somawanshi, A Review on Progression in Synthesis Techniques, Characterization and Catalytic Applications of Transition Metal Oxide Nano Particles. *J. Chem. Lett.*, 5 (2024) 206-220. doi: 10.22034/jchemlett.2024.469255.1217 d) F.M. Omotola, O.O. Olutayo, S.E. Adedunni, Biosynthesis of Iron Oxide Nanoparticles Using Moringa oleifera (Lam) Leaf Extract and Its Anti Plasmodial Studies. *Chem. Res. Technol.*, 2 (2025) 99-107. doi: 10.22034/chemrestec.2025.514186.1043

[12] a) H. Alkadi, A review on free radicals and antioxidants. *Infect. Disord. Drug Targets*, 20 (2020) 16-26.

[13] a) J. Crapo, Oxidative stress as an initiator of cytokine release and cell damage. *Eur. Respir. J.*, 22 (2003) 4s-6s. b) H.K. Abbood, R.R. Hateet, Isolation and identificatio of bacterium Pseudomonas aurginosa from burns and evaluation their ability to green synthesis of silver oxide nanoparticles as Antibacterial agent. *Med. Med. Chem.*, 1 (2024) 129-137. doi: 10.22034/medmedchem.2024.491374.1021 c) E.V. Ishaya, B.K. Modu, J. Yakubu, B.O. Mohammed, Synthesis, characterization, and antimicrobial properties of chromium (III) and iron (III) complexes with schiff base ligands. *J. Chem. Technol.*, 1 (2025) 160-166. doi: 10.22034/jchemtech.2025.548760.1026 d) K.Z. Kolo, N.C. Nwokem, S.E. Abechi, Green Synthesis of Iron Oxide Nanoparticle Using Funaria hygrometrica Extract, and the Study of Its Antimicrobial Activities. *J. Chem. Lett.*, 4 (2024) 222-231. doi: 10.22034/jchemlett.2024.423104.1142

[14] a) M. Muscolo, M.O. Mariateresa, G.T. Giulio, R.M. Mariateresa, Oxidative stress: the role of antioxidant phytochemicals in the prevention and treatment of diseases. *Int. J. Mol. Sci.*, 25 (2024) 3264. b) R.A. Omer, A.Y. Hussein, H.K.I. Sultan, H.K. Ismail, A.F. Hamasdiq, R.O. Kareem, Synthesis and DFT-guided evaluation of PPy-$ZnFe_2O_4$@Fe_3O_4 nanocomposite for pharmaceutical adsorption. *J. Chem. Lett.*, (2026) 240-255. doi: 10.22034/jchemlett.2025.554966.1361 c) E. Askari, A. Alborzi, Ammonium Iron(III) Sulfate as an Eco-friendly Catalyst for the Synthesis of Spirooxindole Dihydroquinazolinone Derivatives. *J. Chem. Technol.*, 1 (2025) 85-89. doi: 10.22034/jchemtech.2025.538321.1014

[15] E.I. Akubugwo, O. Emmanuel, C.N. Ekweogu, O.C. Ugbogu, T.R. Onuorah, O.G. Egeduzu, et al., GC-MS analysis of the phytochemical constituents, safety assessment, wound healing and anti-inflammatory activities of cucurbita pepo leaf extract in rats. *Sci. Pharm.*, 90 (2022) 64.

[16] Kanupriya J, G.A. Sivakumar, Antioxidant potential and Phytochemical analysis of fruit extract of Cucurbita pepo. *Int. J. Curr. Res. Chem. Pharm. Sci.*, 6 (2019) 22-32.

[17] T. Sultana, S. Islam, A. Rahman, A. Jahurul, Antimicrobial and antioxidant properties of the acetone extracts of the leaves of Lagenaria siceraria and Cucurbita pepo. *Food Chem. Adv.*, 3 (2023) 100556.

[18] R. Gyawali, S.A. Ibrahim, Natural products as antimicrobial agents. *Food Control*, 46 (2014) 412-29.

[19] A. Upadhyay, D. Karumathil, I. Upadhyaya, V. Bhattaram, K. Venkitanarayanan, Controlling bacterial antibiotic resistance using plant-derived antimicrobials. *Antibiot. Resist.*, (2016) 205-26.

[20] G.B. Mahady, Medicinal plants for the prevention and treatment of bacterial infections. *Curr. Pharm. Des.*, 11 (2005) 2405-27.

[21] J. Shin, V.S. Prabhakaran, K.S. Kim, The multi-faceted potential of plant-derived metabolites as antimicrobial agents against multidrug-resistant pathogens. *Microb. Pathog.*, 116 (2018) 209-14.

[22] P. Borel, O. Dangles, R.E. Kopec, Fat-soluble vitamin and phytochemical metabolites: Production, gastrointestinal absorption, and health effects. *Prog. Lipid Res.*, 90 (2023) 101220.

[23] M. Joshi, P. Hiremath, J. John, N. Ranadive, K. Nandakumar, J. Mudgal, Modulatory role of vitamins A, B3, C, D, and E on skin health, immunity, microbiome, and diseases. *Pharmacol. Rep.*, 75 (2023) 1096-114.

[24] A. Dattola, M. Silvestri, L. Bennardo, M. Passante, E. Scali, C. Patruno, et al., Role of vitamins in skin health: A systematic review. *Curr. Nutr. Rep.*, 9 (2020) 226-35.

[25] C. Godoy-Parejo, C. Deng, Y. Zhang, W. Liu, G. Chen, Roles of vitamins in stem cells. *Cell. Mol. Life Sci.*, 77 (2020) 1771-91.

[26] O. Dunsin, C. Aboyeji, A. Adekiya, K. Adegbite, O. Adebiyi, R. Bello, et al., Growth, yield, fruit mineral and Vitamin C content of Cucurbita pepo. L as affected by

Organic and NPK fertilizer. *Open Agric.*, 4 (2019) 795-802.
[27] a) C. Fanali, G. D'Orazio, S. Fanali, A. Gentili, Advanced analytical techniques for fat-soluble vitamin analysis. *TrAC-Trend. Anal. Chem.*, 87 (2017) 82-97. b) [Duplicate of 10b removed].
[28] A.K. Kashyap, T. Anju, S.K. Dubey, A. Kumar, S. Kumar, Technological advancements for the analysis of phytochemical diversity in plants. *Phytochemical Genomics*, (2023) 109-25.
[29] A. Balkrishna, M. Joshi, S. Gupta, M.P. Rani, J. Srivastava, P. Nain, et al., Dissecting the natural phytochemical diversity of carrot roots with its colour using high performance liquid chromatography and UV–Visible spectrophotometry. *Heliyon*, 10 (2024).
[30] M.K.A. Sobuj, M.S. Shemul, M.S. Islam, M.A. Islam, S.S. Mely, M.H. Ayon, et al., Qualitative and quantitative phytochemical analysis of brown seaweed Sargassum polycystum collected from Bangladesh with its antioxidant activity determination. *Food Chem. Adv.*, 4 (2024) 100565.
[31] V. Soni, P. Raizada, P. Singh, H.N. Cuong, S. Rangabhashiyam, A. Saini, et al., Sustainable and green trends in using plant extracts for the synthesis of biogenic metal nanoparticles toward environmental and pharmaceutical advances: A review. *Environ. Res.*, 202 (2021) 111622.
[32] S. León-Silva, F. Fernández-Luqueño, F. López-Valdez, Silver nanoparticles (AgNP) in the environment: a review of potential risks on human and environmental health. *Water Air Soil Pollut.*, 227 (2016) 306.
[33] C. Hano, B.H. Abbasi, Plant-based green synthesis of nanoparticles: Production, characterization and applications. *MDPI*, (2021) 31.
[34] A. Kaushik, R.K. Singh, P.K. Tyagi, Green Synthesized Nanoparticle Based Drug Delivery: Recent Trends and Future Prospects. *Precis. Nanomed.*, 6 (2023) 1109-31.
[35] M.A. Irshad, A. Hussain, I. Nasim, R. Nawaz, A.A. Al-Mutairi, S. Azeem, et al., Exploring the antifungal activities of green nanoparticles for sustainable agriculture: a research update. *Chem. Biol. Technol. Agric.*, 11 (2024) 133.
[36] A.I. Osman, Y. Zhang, M. Farghali, A.K. Rashwan, A.S. Eltaweil, E.M. Abd El-Monaem, et al., Synthesis of green nanoparticles for energy, biomedical, environmental, agricultural, and food applications: A review. *Environ. Chem. Lett.*, 22 (2024) 841-87.
[37] R.K. Dubey, S. Shukla, Z. Hussain, Green Synthesis of Silver Nanoparticles; A Sustainable Approach with Diverse Applications. *Chin. J. Appl. Physiol.*, 2023 (2023) e20230007.
[38] A.A. Amin, S. Ekin, A. Bakır, D. Yıldız, Antioxidant properties of Lycianthes rantonnetii and contents of vitamin and element. *Int. J. Second. Metab.*, 9 (2022) 194-207.
[39] S. Jäger, M. Beffert, K. Hoppe, D. Nadberezny, B. Frank, A. Scheffler, Preparation of herbal tea as infusion or by maceration at room temperature using mistletoe tea as an example. *Sci. Pharm.*, 79 (2011) 145-56.
[40] M. Contini, S. Baccelloni, R. Massantini, G. Anelli, Extraction of natural antioxidants from hazelnut (Corylus avellana L.) shell and skin wastes by long maceration at room temperature. *Food Chem.*, 110 (2008) 659-69.
[41] A.F. Abdullah, S.J. Piro, N.H. Ali, A.F. Qader, A.A. Amin, R.A. Omer, et al., Cucurbita pepo Seed Extract and Green-Synthesized Silver Nanoparticles: Antioxidant, Phytochemical, and Antibacterial Properties. *J. Mol. Eng. Mater.*, (2025) 2550027.
[42] N. Gamez-Meza, J. Noriega-Rodriguez, L. Medina-Juarez, J. Ortega-Garcia, R. Cazarez-Casanova, O. Angulo-Guerrero, Antioxidant activity in soybean oil of extracts from Thompson grape bagasse. *J. Am. Oil Chem. Soc.*, 76 (1999) 1445-7.
[43] A.F. Qader, M. Yaman, Phytochemical Profile, Antioxidant Capacity, and Chromatographic Separation of Sumac (Rhus Coriaria L.) Extract. *J. Mol. Eng. Mater.*, (2025) 2550026.
[44] A.F. Qader, M. Yaman, Blackberry (Rubus fruticosus L.) Fruit Extract Phytochemical Profile, Antioxidant Properties, Column Chromatographic Fractionation, and High-performance Liquid Chromatography Analysis of Phenolic Compounds. *ARO-Sci. J. Koya Univ.*, 11 (2023) 43-50.
[45] E. Urgeova, L. Polivka, Secondary metabolites with antibacterial effects from leaves of different hop cultivars during vegetal periods. *Nova Biotechnol.*, 9 (2009) 327-32.
[46] B. Dimitrios, Sources of natural phenolic antioxidants. *Trends Food Sci. Technol.*, 17 (2006) 505-12.
[47] R. Tundis, F. Menichini, M. Bonesi, F. Conforti, G. Statti, F. Menichini, et al., Antioxidant and hypoglycaemic activities and their relationship to phytochemicals in Capsicum annuum cultivars during fruit development. *LWT-Food Sci. Technol.*, 53 (2013) 370-7.
[48] H. Rodrigues, Y. Diniz, L. Faine, C. Galhardi, R. Burneiko, J. Almeida, et al., Antioxidant effect of saponin: potential action of a soybean flavonoid on glucose tolerance and risk factors for atherosclerosis. *Int. J. Food Sci. Nutr.*, 56 (2005) 79-85.
[49] E.A. Shalaby, S.M. Shanab, Comparison of DPPH and ABTS assays for determining antioxidant potential of water and methanol extracts of Spirulina platensis. (2013).
[50] M. Karatepe, Simultaneous determination of ascorbic acid and free malondialdehyde in human serum by HPLC-UV. *LCGC North Am.*, 22 (2004) 362-5.
[51] G. Catignani, J. Bieri, Simultaneous determination of retinol and alpha-tocopherol in serum or plasma by liquid chromatography. *Clin. Chem.*, 29 (1983) 708-12.
[52] V. Parashar, R. Parashar, B. Sharma, A.C. Pandey, Parthenium leaf extract mediated synthesis of silver nanoparticles: a novel approach towards weed utilization. *Dig. J. Nanomater. Biostruct.*, 4 (2009).
[53] D. Kumar, S. Arora, M. Danish, Plant based synthesis of silver nanoparticles from Ougeinia oojeinensis leaves extract and their membrane stabilizing, antioxidant and antimicrobial activities. *Mater. Today Proc.*, 17 (2019) 313-20.
[54] L.M. Ng, R. Simmons, Infrared spectroscopy. *Anal. Chem.*, 71 (1999) 343-50.
[55] Y. Sadef, T. Javed, R. Javed, M. Mahmood, M.S. Alwahibi, M.S. Elshikh, et al., Nutritional status, antioxidant activity and total phenolic content of different fruits and vegetables' peels. *PLoS One*, 17 (2022) e0265566.

[56] S. Chigurupati, Y. AlGobaisy, B. Alkhalifah, A. Alhowail, S. Bhatia, S. Das, et al., Antioxidant and antidiabetic potentials of Cucurbita pepo leaves extract from the gulf region. *Rasayan J. Chem.*, 14 (2021) 2357-62.

[57] I. Guleria, A. Kumari, M.A. Lacaille-Dubois, A.K. Saini, V. Kumar, R.V. Saini, et al., In-vitro antimicrobial, antioxidant, anti-inflammatory, and cytotoxic activities of Populus ciliata bark and leaves: A comparative study. *S. Afr. J. Bot.*, 148 (2022) 238-50.

[58] L. Kolarević, E. Horozić, Z. Ademović, E.C. Kozarević, Investigation of Polyphenol Content and Antioxidative Activity of Cucurbita pepo L. Leaf Extracts Obtained by Ultrasonic Extraction. *Int. Res. J. Pure Appl. Chem.*, 24 (2023) 1-8.

[59] J.S. Boeing, É.O. Barizão, B.C. e Silva, P.F. Montanher, V. de Cinque Almeida, J.V. Visentainer, Evaluation of solvent effect on the extraction of phenolic compounds and antioxidant capacities from the berries: application of principal component analysis. *Chem. Cent. J.*, 8 (2014) 1-9.

[60] K. Jomova, M. Valko, Importance of iron chelation in free radical-induced oxidative stress and human disease. *Curr. Pharm. Des.*, 17 (2011) 3460-73.

[61] R.C.G. Corrêa, J.A.A. Garcia, V.G. Correa, T.F. Vieira, A. Bracht, R.M. Peralta, Pigments and vitamins from plants as functional ingredients: Current trends and perspectives. *Adv. Food Nutr. Res.*, 90 (2019) 259-303.

[62] M. Srbinoska, N. Hrabovski, V. Rafajlovska, S. Sinadinović-Fišer, Characterization of the seed and seed extracts of the pumpkins Cucurbita maxima D. and Cucurbita pepo L. from Macedonia. *Maced. J. Chem. Chem. Eng.*, 31 (2012) 65-78.

[63] B. Kulczyński, A. Gramza-Michałowska, The profile of secondary metabolites and other bioactive compounds in Cucurbita pepo L. and Cucurbita moschata pumpkin cultivars. *Molecules*, 24 (2019) 2945.

[64] R. Rajan, K. Chandran, S.L. Harper, S.I. Yun, P.T. Kalaichelvan, Plant extract synthesized silver nanoparticles: An ongoing source of novel biocompatible materials. *Ind. Crops Prod.*, 70 (2015) 356-73.

[65] P. Logeswari, S. Silambarasan, J. Abraham, Synthesis of silver nanoparticles using plants extract and analysis of their antimicrobial property. *J. Saudi Chem. Soc.*, 19 (2015) 311-7.

[66] D. Das, R. Ghosh, P. Mandal, Biogenic synthesis of silver nanoparticles using S1 genotype of Morus alba leaf extract: characterization, antimicrobial and antioxidant potential assessment. *SN Appl. Sci.*, 1 (2019) 1-16.

[67] S. Bhakya, S. Muthukrishnan, M. Sukumaran, M. Muthukumar, Biogenic synthesis of silver nanoparticles and their antioxidant and antibacterial activity. *Appl. Nanosci.*, 6 (2016) 755-66.

[68] S.S. Shankar, A. Rai, A. Ahmad, S. Sastry, Rapid synthesis of Au, Ag, and bimetallic Au core–Ag shell nanoparticles using Neem (Azadirachta indica) leaf broth. *J. Colloid Interface Sci.*, 275 (2004) 496-502.

[69] J. Rojas, C. Londoño, Y. Ciro, The health benefits of natural skin UVA photoprotective compounds found in botanical sources. *Int. J. Pharm. Pharm. Sci.*, 8 (2016) 13-23.

[70] S.B. Aziz, R.B. Marif, M. Brza, A.N. Hassan, H.A. Ahmad, Y.A. Faidhalla, et al., Structural, thermal, morphological and optical properties of PEO filled with biosynthesized Ag nanoparticles: New insights to band gap study. *Results Phys.*, 13 (2019) 102220.

[71] T. Amin, H. Naik, S.Z. Hussain, A. Jabeen, M. Thakur, In-vitro antioxidant and antibacterial activities of pumpkin, quince, muskmelon and bottle gourd seeds. *J. Food Meas. Charact.*, 12 (2018) 182-90.

[72] K. Roy, C. Sarkar, C. Ghosh, SINGLE-STEP NOVEL BIOSYNTHESIS OF SILVER NANOPARTICLES USING CUCUMIS SATIVUS FRUIT EXTRACT AND STUDY OF ITS PHOTCATALYTIC AND ANTIBACTERIAL ACTIVITY. *Dig. J. Nanomater. Biostruct.*, 10 (2015).

[73] M. Tasiu, Y. Abdulmumin, T. Abdulmumin, M. Murtala, A. Shehu, A. Abubakar, et al., Antimicrobial evaluation of biologically synthesized silver nanoparticles using aqueous peel extracts of guava (Psidium guavaja) and pumpkin (cucurbita pepo). *Asian J. Biotechnol. Genet. Eng.*, 5 (2022) 20-9.

[74] N. Dali, S. Dali, A. Chairunnas, H.A.M. Amalia, S.A.A. Puspitasari, Synthesis of the BETAC4ND5 ionophore from pt-butylcalix arene ethylesteramide. *AIP Conf. Proc.*, (2022).

[75] V. Ahluwalia, Infrared Spectroscopy. *Instrumental Methods of Chemical Analysis*, (2023) 179-231.

[76] K.I. Takei, R. Takahashi, T. Noguchi, Correlation between the hydrogen-bond structures and the C□ O stretching frequencies of carboxylic acids as studied by density functional theory calculations. *J. Phys. Chem. B*, 112 (2008) 6725-31.

[77] A.G. Al Lafi, FTIR spectroscopic analysis of ion irradiated poly (ether ether ketone). *Polym. Degrad. Stab.*, 105 (2014) 122-33.

[78] J. Coates, Interpretation of infrared spectra, a practical approach. *Encycl. Anal. Chem.*, 12 (2000) 10815-37.